Microporous and Mesoporous Materials 216 (2015) 127–132

Contents lists available at ScienceDirect

Microporous and Mesoporous Materials

journal homepage: www.elsevier.com/locate/micromeso

Deuterium/hydrogen permeation through different molecular sieve membranes: ZIF, LDH, zeolite

S. Friebe, N. Wang, L. Diestel, Y. Liu, A. Schulz, A. Mundstock, J. Caro*

Institute of Physical Chemistry and Electrochemistry, Leibniz University Hannover, Callinstraße 22, 30167 Hannover, Germany

ARTICLE INFO

Article history:
Received 28 November 2014
Received in revised form
25 March 2015
Accepted 29 March 2015
Available online 4 April 2015

Keywords:
Deuterium/hydrogen separation
Permeation
Zeolite membrane
ZIF membrane

ABSTRACT

Different molecular sieve membranes have been evaluated in the separation of deuterium (D_2)/hydrogen (H_2) mixtures. Both the single gases and the binary D_2/H_2 mixture have been permeated at room temperature through supported Metal Organic Framework (MOF) membranes (ZIF-8 and ZIF-90) as well as through supported zeolite (SOD, LTA, FAU) and layered double hydroxide (LDH) membranes. Also the D_2/H_2 permeation through the non-coated bare α-Al_2O_3 supports, and pressed graphite discs has been studied. Since the molecular mass of D_2 is twice the mass of H_2, and D_2 is slightly smaller than H_2, D_2 should show higher single component permeability than H_2 because of its favored adsorption and diffusion compared with H_2. For the MOF membranes (ZIF-8 and ZIF-90) as well as the LDH membrane, the single gas D_2 permeabilities are indeed by the factor of 3 larger than those of H_2 at room temperature. However, due to strong molecular interaction, no separation is found for the equimolar D_2/H_2 mixture. For comparison, we also studied the permeation of He/D_2. Since these mixture components are of the same molecular mass and almost the same size, no separation can be expected and no separation has been found.

1. Introduction

The stable hydrogen isotope deuterium (D_2) is used in a variety of applications like nuclear fusion or isotopic tracing. Based on the limited availability [1] on earth and the versatile applicability of D_2 it is necessary to develop low-cost separation processes. However, in consequence of the almost same size and the similar physical and chemical behavior of the hydrogen isotopes, D_2/H_2 separation becomes a challenging task. Therefore, just a few methods, namely cryogenic distillation or electrolysis of water, are qualified at present for large scale hydrogen isotope separation. However, the main disadvantage of these methods is their expensiveness due to their low separation factors (1.5 in distillation and 2.3 in electrolysis) [2]. Another interesting principle for the isotope separation is the adsorptive quantum sieving (QS) effect at temperatures around 70 K and lower [3,4]. This effect occurs when the difference between molecular size and the pore diameter is in the range of the de-Broglie wavelength of hydrogen. If these conditions are fulfilled, the lighter isotope H_2 will be impeded more than the heavier D_2 in the pore system due to the differences between their zero point energy (ZPE). The lower the temperature gets, the higher are the differences between the diffusion coefficients of the isotopes. This effect results in a separation of the isotopes what was already investigated by different groups such as Beenakker et al. [4] or Heine et al. [5]. Nevertheless, the drawback with this method is the stringent necessity of the cooling to low temperatures. Otherwise the effect of QS cannot be obtained.

Here we present another separation concept based on the different diffusion and adsorption behavior of D_2 and H_2 at room temperature. On the one hand, D_2 is slightly smaller than H_2. As a result of this, the D_2 diffusion coefficient should be higher than the H_2 diffusion coefficient. On the other hand, D_2 is twice heavier than H_2, which affects the adsorption selectivity resulting in a higher adsorbed amount of D_2. This adsorption concept was followed in previous quantum sieving experiments at much lower temperature [6]. The two effects, better D_2 adsorption and higher D_2 diffusivity, should cooperate in the case of membrane permeation. As a rough estimate for membrane selectivity, we can assume that.

Membrane selectivity $\approx$ diffusion selectivity $\times$ adsorption selectivity [7,8]. (1)

---

* Corresponding author.
E-mail address: juergen.caro@pci.uni-hannover.de (J. Caro).

http://dx.doi.org/10.1016/j.micromeso.2015.03.034
1387-1811/

Following this concept of different adsorption and diffusion behavior of the hydrogen isotopes, we can expect a permeative separation of a D_2/H_2 mixture even at room temperature with D_2 as the preferentially permeated component.

For the evaluation of this concept, we selected several nanoporous membranes with proven molecular sieve separation ability developed in our group: Metal Organic Framework (MOF) materials of type ZIF (zeolitic imidazolate framework), zeolites, layered double hydroxide (LDH) and pressed graphite. Especially MOFs are promising membrane materials because of their property to tune their adsorption properties (pore size [9], linker functionalization [10], specific gas adsorption [11]). Based on their very high porosity, MOFs show enormous specific surface areas which can be used for gas storage by physisorption [12]. Teufel et al. demonstrated the potential of MOF's in adsorptive hydrogen isotope separation [13].

The pressed graphite membranes should also show interesting separation behavior due to a different D_2/H_2 adsorption selectivity. For instance, Jiao et al. [14] and Zhang et al. [15] studied the adsorptive hydrogen isotope separation on carbon materials based on quantum sieving with a favored adsorption selectivity of D_2. The gas transport through a graphite membrane proceeds through the grain boundaries as shown in Ref. [16]. Therefore, the pressed graphite membrane is a good candidate to investigate separation behavior independent of a molecular sieve pore system.

However, zeolites with their rigid pore system separate gases by molecular sieving rather than by adsorptive interactions. Since D_2 is only slightly smaller than H_2, we expect that most of the zeolite membranes will not separate the D_2/H_2 mixture since their pore size is not exact at 2.9 Å. As a proof of our concept, also the permeation of the hydrogen isotopes through the neat α-Al_2O_3 support has been studied. Whereas for the MOF and zeolite membranes a more or less pronounced D_2 over H_2 selectivity is anticipated, for the macroporous support a separation in the range of the Knudsen factor

$$\alpha(D_2/H_2) \approx \sqrt{\frac{M(H_2)}{M(D_2)}} \approx \sqrt{0.5} \approx 0.7$$

is expected. This behavior occurs if the pores are bigger than the diameter of the gases and if there are no special interactions with the pore system. In this case collisions with the walls of the pore system appear more frequently than collisions between the gas molecules, and the lighter gas should pass the pore system easier [17,18].

2. Experimental

2.1. Preparation of supported ZIF-90, ZIF-8 and LDH membranes

For hydrogen isotope permeation, different types of membranes were prepared. The syntheses of these membranes were done following recipes reported elsewhere (ZIF-90 [19], ZIF-8 [20], LDH [21,22], pressed graphite [16], FAU [23], SOD [24], LTA [23,25]). Here, we give only a short description of the three most promising membranes according to the single component tests. All supported membranes were prepared on α-alumina supports (70 nm pores in top layer, Fraunhofer IKTS, former Hermsdorfer HITK, Germany).

2.1.1. Synthesis of ZIF-90 membrane

The α-Al_2O_3 supports were functionalized with 0.46 g APTES (3-aminopropyltriethoxysilane, Sigma Aldrich) in 10 mL toluene at 110 °C for 2 h, followed by several washing steps with toluene. Afterward the disks were placed horizontally in a Teflon lined autoclave. A solution of 0.43 g $Zn(NO_3)\cdot 4H_2O$ and 0.23 g imidazole-2-carboxyaldehyde (Sigma Aldrich) in 24 mL DMF was then filled into a vessel and sealed. Then the autoclave was heated to 100 °C in a convection oven for 18 h. After the synthesis the membrane was washed with DMF and dried at 60 °C overnight.

2.1.2. Synthesis of ZIF-8 membrane

The ZIF-8 membranes were produced by the secondary growth method. Therefore a solution of 0.12 g sodium hydrogen carbonate, 1.20 g polyethyleneimine (Sigma Aldrich, ~50% in water, 4 wt.%), 0.80 g ZIF-8 nanoparticles in 30 mL water was prepared. This solution was used to produce a layer of seeding crystals on top of the supports by dip coating. The dipping parameters were set as following: up speed = 200 mm min^{-1}, down speed = 300 mm min^{-1}, lower delay = 10 s, and upper delay = 3 min. After the coating process the supports were dried overnight at room temperature. For the secondary growth process, 0.54 g $ZnCl_2$ (3.94 mmol, 1 eq.), 0.49 g 2-methylimidazole (5.92 mmol, 1.5 eq.) and 0.27 g sodium formate (3.94 mmol, 1 eq.) (Sigma Aldrich) were solved in 80 mL methanol. This solution was filled in a 200 mL Teflon lined autoclave and one of the seeded supports was put vertically in the solution. The autoclave was heated in the microwave oven with a heating rate of 7.5 °C min^{-1} at 100 °C for 1.5 h. After the autoclave was cooled down to room temperature, the membrane was washed with 20 mL methanol and dried overnight at room temperature.

2.1.3. Synthesis of LDH membrane

The precursor solution was prepared by adding 5.8 g $Ni(NO_3)_2\cdot 6H_2O$ (98.0 wt. %, Merke) and 4.8 g NH_4NO_3 (Aldrich, 98.0 wt.%) into 100 mL CO_2-saturated water (Vitalitasia Classic, containing saturated CO_2). Consequently 10 mL 1 wt.% $NH_3\cdot H_2O$ (Aldrich, 28 wt.%) was added dropwise into the aqueous solution and stirred in an ice bath for 10 min. After that a γ-Al_2O_3-modified α-alumina support was vertically placed into a 50 mL Teflon-lined stainless vessel. Then 35 mL of aqueous solution was poured into the vessel and sealed. The vessel was put into convective oven with the temperature pre-heated to 85 °C. After an elapsed time of 40 h, it was taken out and cooled to room temperature in air. Finally the membrane was taken out and washed with copious of DDI water. Before gas separation measurement, the membrane was dried in a convective oven at 60 °C for 12 h.

2.2. Electron microscopy

The Scanning Electron Microscopy (SEM) studies of the membranes were done with a field-emission electron microscope (JEOL JSM-6700F). The accelerating voltage was set to 2 kV and the working distance was 8 mm.

2.3. Gas permeation measurements

Our assumptions of the permeation properties are evaluated by single gas and mixed gas separation measurements. The membranes were sealed in the permeation cell with Viton O-rings (FKM 70 Vi 370). In single gas measurements gas chromatography (Agilent Technologies 7890B) was applied. Mixed gas separation analysis was done by mass spectrometry (OMNISTAR GSD QMS 200 Quadrupol). Some membranes were tested with vacuum on the permeate side to minimize the effect of counter diffusion which can take place in Wicke-Kallenbach measurements (cf. the influence of the pressure difference Δp over the membrane in Table 1). In this case, the permeate side was evacuated by a vacuum pump (Pfeiffer MVP 015-4). Fig. 1 shows the measurement setup for both single and mixed gas permeation. For mixed gas permeation, the

Table 1
Single gas ideal separation factors SF, mixed gas separation factors α and measurement conditions for the molecular sieve membranes under study. For the Ideal separation factors SF D_2/H_2 and single gas permeabilities see Fig. 3.

Membranes	SF D_2/H_2	α D_2/H_2	T/°C	Δp/bar
Supported ZIF-90	3.6[a,b]	1.2[a,b]	25	1
Supported ZIF-8	3.5[a,b]	1.1[a,b]	25	1
Supported LDH	3.2[a]	1.2[a]	150	0
Pressed graphite	2.1[b]	0.8[b]	25	1
Supported FAU[c]	1.1[a]	–	25	0
Supported SOD[c]	1.1[a]	0.8[a]	25	0
Supported LTA[c]	1.0[a]	1.0[a]	25	0
α-Al_2O_3 support	0.8[a]	1.0[a]	25	0
Polymers [27,28]	–	0.9	–	–
Metals [29–31]	–	0.7	–	–

[a] Feed side 1 bar, sweep side 1 bar, Wicke-Kallenbach technique with N_2 as sweep gas.
[b] Feed side 1 bar, sweep side ≈ 0.1 bar (vacuum), N_2 to sweep into GC.
[c] The zeolite membranes FAU, LTA and SOD were in the Na^+ cationic state.

permeated gas was stored and analyzed off line by injection into the mass spectrometer using syringes.

3. Results and discussion

Different MOF and zeolite membranes—developed in our group previously with proven gas separation performance—have been evaluated in the D_2/H_2 permeation. On the one hand, supported MOF membranes of type ZIF-8 and ZIF-90 have been selected for the D_2/H_2 separation. We expect an adsorption based selectivity because of the strong interaction of hydrogen with the MOF framework [11,26] rather than molecular sieving (pore sizes neglecting framework flexibility are 3.4 Å (ZIF-8) and 3.5 Å (ZIF-90), i.e. larger than H_2 (2.9 Å) and D_2 (2.89 Å). On the other hand, different zeolite LTA, SOD, NaX and LDH membranes with a more rigid pore system and a less pronounced interaction with hydrogen were selected to study the separation behavior of the hydrogen isotopes. To examine separation processes that are independent from the pore system of the material, a pressed graphite membrane was chosen, because in this case the permeation takes place through the grain boundaries of the pressed graphite flakes. Also the bare α-Al_2O_3 support with hierarchical structure was used for comparison to study the hydrogen isotope separation on a mesopore membrane without specific adsorptive interaction with hydrogen.

3.1. Synthesis of supported ZIF and LDH membranes

Fig. 2 shows the cross sections of the three membranes with the highest ideal separation factors as derived from single components permeation studies (cf. Table 1): ZIF-8, ZIF-90, LDH, and the bare α-Al_2O_3 support. The SEM shows dens and homogeneous layers with well intergrown crystals for all membranes under study. The thicknesses of the ZIF membranes are about 10 μm, whereas the LDH membrane is about 5 μm thick.

3.2. Single gas permeation

The comparison of the single gas permeation data (c.f. Table 1, Fig. 3) indicates that MOFs show the highest ideal separation factors SF for a D_2/H_2 gas mixture with ZIF-90: SF ≈ 3.6, and ZIF-8: SF ≈ 3.5. LDH and pressed graphite membranes show ideal selectivities SF for the hydrogen isotopes D_2/H_2 with 3.2 (LDH) and 2.1 (graphite). However, the different supported zeolite membranes SOD, LTA, FAU and also the bare α-Al_2O_3 support which was used for the preparation of the supported MOF, zeolite and LDH membranes, show ideal separation factors SF D_2/H_2 ≈ 1.1–0.8 which are slightly larger than the Knudsen factor Kn (D_2/H_2 ≈ 0.7). Fig. 3 shows the ideal separation factors SF D_2/H_2 and the corresponding single gas permeabilities for the different molecular sieve membranes under study. Table 1 gives the ideal separation factors SF D_2/H_2 and the real mixed gas separation factors α D_2/H_2 measured for the equimolar mixture D_2/H_2. Also the permeation conditions and the separation performances of common polymer membranes and metal membranes in the D_2/H_2 separation are given for comparison in Table 1. To avoid artifacts from the permeation methods applied, we have used different measurement methods to detect gas permeation: Both in single and mixed gas permeation, we used (a) Wicke-Kallenbach method with equal pressures of 1 bar on feed and permeate side and N_2 as feed gas, and (b) reduced pressure (vacuum) of ≈0.1 bar on the permeate side.

At first sight, the single gas permeation data from Table 1 and Fig. 3 seem to prove that our expectations are fulfilled: For the best membranes (ZIF-90, ZIF-8, LDH), the single gas permeabilities of D_2 at room temperature are up to the factor of 3 higher than those of H_2. The ranking starts with the MOF membranes with ideal

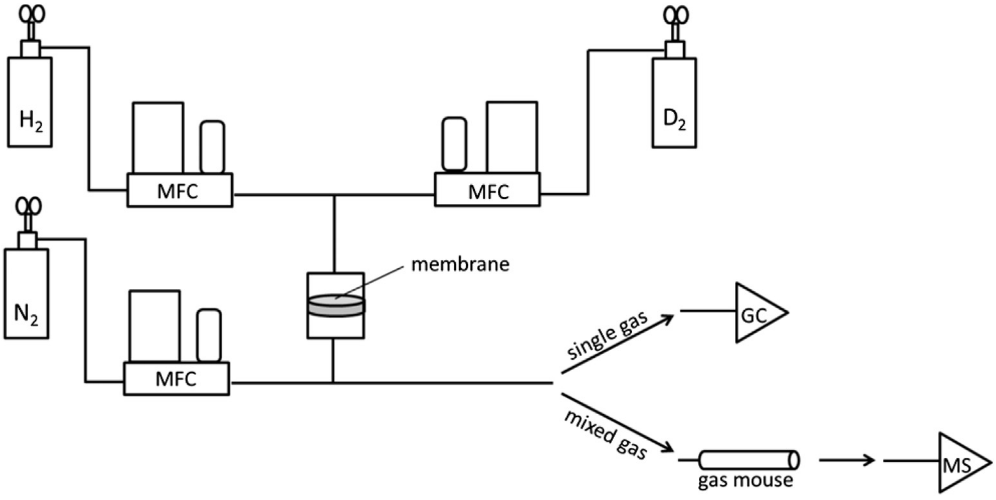

Fig. 1. Measurement setup for single and mixed gas permeation.

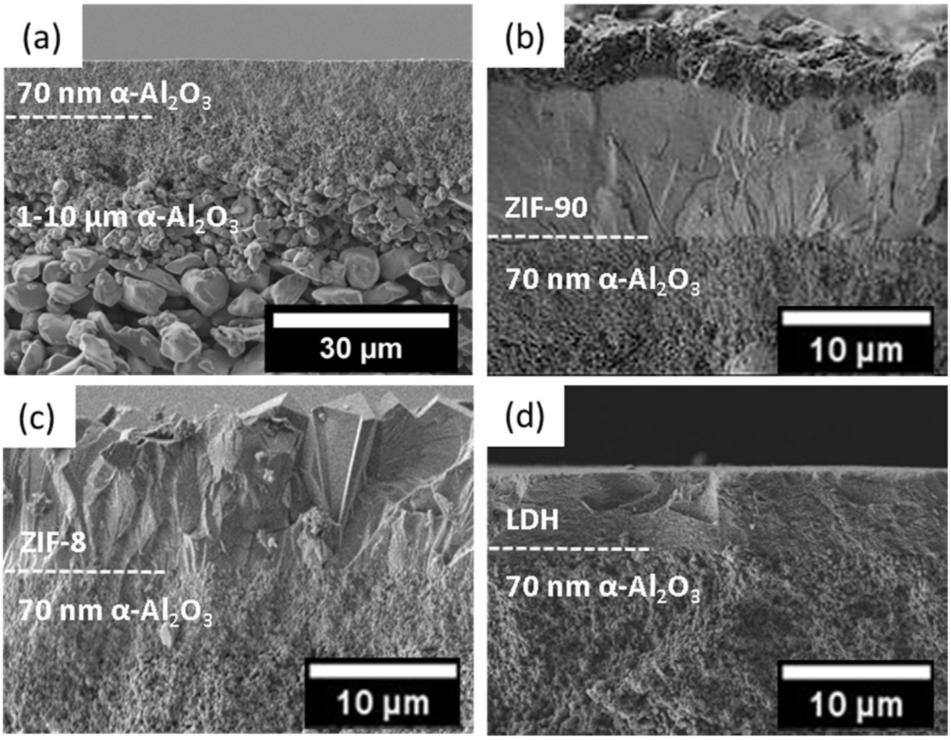

Fig. 2. Cross section of the bare α-Al_2O_3 support (a), ZIF-90 membrane (b), ZIF-8 membrane (c) and LDH membrane (d). Note that on top of the ZIF-90 membrane there is a sediment layer since the synthesis was made horizontally. Since we have no foreign XRD signals (not shown here), this layer is either ZIF-90 or X-ray amorphous.

separation factors D_2/H_2 of around 3.5 and end ends up at the bare α-Al_2O_3 support with a separation factor of 0.8 which is near to the Knudsen factor. The results from the single gas permeations studies indicate that we can expect on our MOF membranes mixed gas separation factors α which are about five times higher than the Knudsen value. It has to be noted that also on most common polymers or metal alloys a mixed gas selectivity near to the Knudsen factor is observed. We explain this enhanced D_2 permeation in comparison with that of H_2 by the stronger D_2 adsorption and its higher diffusivity in the different ZIFs. The enhanced D_2 permeability on the pressed graphite membrane can be attributed to a different adsorption/desorption behavior of D_2 and H_2 on carbon materials [6,12]. However, no remarkable differences in the D_2 and H_2 single gas permeabilities were found for the zeolite membranes FAU, SOD, LTA. As expected, the bare α-Al_2O_3-support with a top layer with 70 nm pores (determined by Fraunhofer IKTS, Germany) shows Knudsen behavior, that is to say that the H_2 permeability is by the factor of ≈1.25 larger than that of D_2

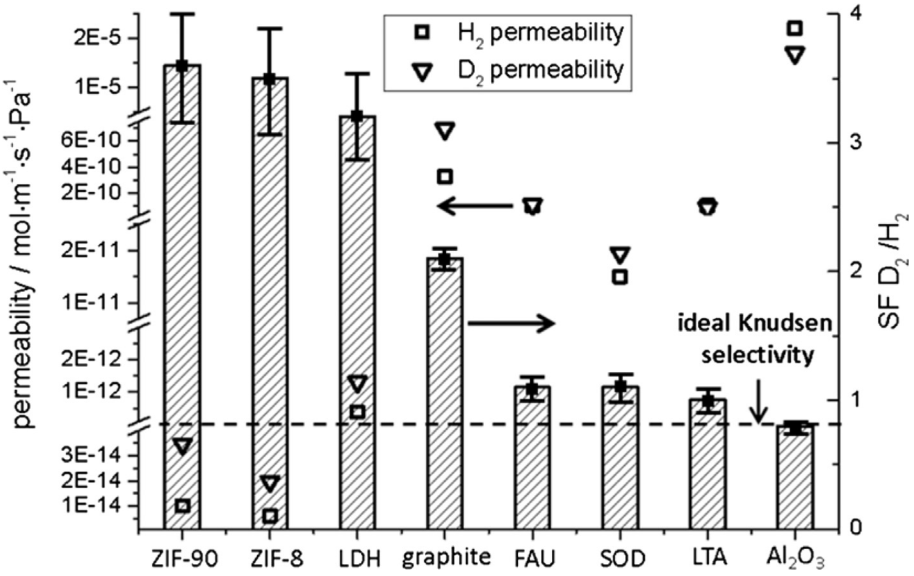

Fig. 3. Ideal separation factors SF D_2/H_2 and single gas permeabilities for the different membranes under study including error bars for the separation factors. For the measurement conditions, see Table 1.

(Knudsen factor: 1.41). It can be summarized, that these single gas studies give a consistent picture and thus it is anticipated that we can obtain a similar selectivity for the D_2/H_2 mixtures.

We studied as well the permeation of He and D_2 on the two membranes ZIF-90 and ZIF-8 as well as for comparison on the alumina support. He and D_2 are of the same molecular mass and of similar size. As expected, the ideal separation factor SF is near unity (Fig. 4) and binary the mixture He/D_2 cannot be separated.

3.3. *Mixed gas permeation*

In the mixed gas permeation, equimolar D_2/H_2 mixtures have been used. The permeated gas was filled into a gas mouse and then analyzed off-line by mass spectrometry. Injection was done by a syringe. The D_2/H_2 mixed gas separation factor α in Table 1 is around 1 for all membranes, which means that—despite the optimistic prediction from the single gas permeation studies—no separation takes place at room temperature.

If the D_2/H_2 system would behave "normal", from the different D_2 and H_2 single component permeabilities we should expect a mixed gas separation factor α of the order of up to 3 (ideal SF as ratio of single component permeabilities, Table 1), but no separation could be detected for the binary mixture D_2/H_2. It is usual that the separation performance of industrial polymer membranes is predicted for their practice-relevant application on the basis of single gas permeation data. However, when a mixture permeates through a porous membrane, there exists coupling effects which slow down a mobile component by a less mobile species. There is some experimental evidence that a molecule which is strongly adsorbed on a special sorption site can slow down the mobility of a more mobile component. As an example, the branched hexane isomers are preferentially adsorbed in the channel intersections of the MFI structure while n-hexane adsorbs at low loadings in the channel segments. The single component sorption uptake rate of n-hexane was found to be one order of magnitude higher than that of 2,2 dimethylbutane. However, in the case of sorption uptake of the binary mixture, both components enter the MFI at the same low sorption rate [32]. In an MAS pulsed field gradient NMR study, the selective adsorption of i-butane in the channel intersections brought the self-diffusion of n-butane to a stand-still because of the blocking of the intersections by the i-butane [33,34]. Krishna called this effect "slowing down of more-mobile-less-strongly-adsorbed molecules by tardier-more-strongly-adsorbed-partner species" [35].

The degree of correlation is strongly dependent on structure parameters like pore size, topology and connectivity, but also on such experimental parameters like pore filling and temperature. We expected that the extent of this correlation is low for the D_2/H_2 mixture and structures with cages connected by narrow windows where molecules without specific interaction with the host do not occupy certain adsorption sites like in ZIF-8, ZIF-90, LTA and SOD. The molecules perform uncorrelated motions inside the cavity and hop through the narrow window into the next cage by an uncorrelated activated jump. For such cage/window structures and no specific host/guest interaction, the Maxwell–Stefan formulation for mixture permeation [36] allow a quantitative prediction of the mixture permeation.

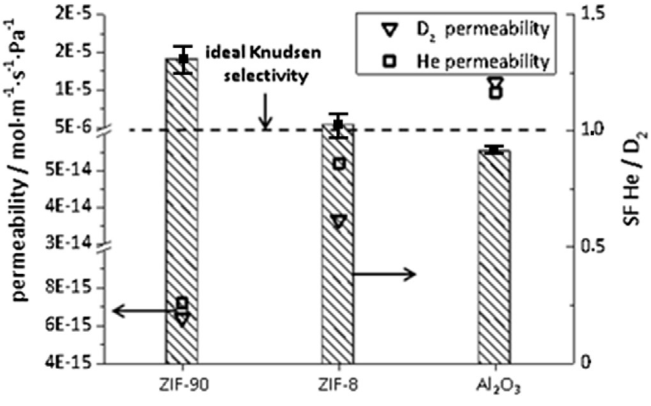

Fig. 4. Ideal separation factors SF He/D_2 and single gas permeabilities at room temperature and Wicke-Kallenbach technique for the different membranes under study including error bars for the separation factors.

Since (i) H_2 and D_2 are (at room temperature) not strongly adsorbed on special sites with long residence times, and (ii) the hydrogen isotopes should perform uncorrelated motions within the cage/window like structure of ZIF-8, ZIF-90, LTA and SOD, with uncorrelated activated jumps through windows [37], the strong correlation of the H_2 and D_2 permeation is difficult to understand. Obviously, the high molecular mobility of the hydrogen isotopes inside the pore structure leads to an equilibration of their mobility as a result of molecule–molecule and molecule–wall collisions. Such pronounced fluid–fluid interaction between the two isotopes H_2 and D_2 at increased pore filling and with increasing temperature as observed in neutron scattering and molecular dynamics studies [38]. Also in a previous study we found that in the slit pores of pressed graphite the diffusivity of the mobile component H_2 is slowed down in the binary mixture with CO_2 and as a result the real mixed gas separation factor is much lower than that one predicted by the ideal selectivity SF [16]. It seems to be a common feature that at high pore filling the adsorbed components of a mixture do not behave like the single components, that is to say, the highly mobile component is slowed down by the less mobile component as observed in previous studies As a consequence, in some industrially driven R&D projects—despite promising single gas results—the mixture permeation results were by the end disappointing [39,40]. We ascribe the non-separability of a D_2/H_2 mixture on our pore membranes at 1 bar feed pressure to this equilibration effect.

4. Conclusions

The permeation behavior of the hydrogen isotopes D_2 and H_2 through different porous membranes was investigated and detected by gas chromatography and mass spectrometry at room temperature. The single gas permeation shows by the factor of up to 3 higher D_2 permeabilities on the MOF membranes ZIF-8 and ZIF-90 in comparison with H_2. This finding is explained with differences in the adsorption and diffusion behavior between the two hydrogen isotopes. Also LDH and pressed graphite membranes show ideal separation factors D_2/H_2 larger than the Knudsen factor. It speaks for the consistency of the single component studies that the neat support without MOF, zeolite or LDH top layer, behaves Knudsen-like with an ideal separation factor SF $D_2/H_2 \approx 0.8$, i.e. SF $H_2/D_2 \approx 1.25$ (Knudsen factor $H_2/D_2 = 1.41$).

However, the mixed gas permeation of the isotope mixture D_2/H_2 at room temperature shows no separation, i.e. the separation factor α $D_2/H_2 \approx 1$ was found for all membranes under study. We explain this surprising finding with fluid–fluid interaction at increased pore filling.

To validate the D_2/H_2 measurements, we studied also He/D_2. For this mixture, the components are of the same molecular mass and almost the same size, and therefore no separation can be expected and no separation has been found.

We want to alert all colleagues in the field of permeation, that in the case (nano) porous membranes because of strong molecule–molecule and molecule–wall interactions, single gas measurements can predict a wrong mixture separation performance.

Acknowledgments

This work is part of the DFG Priority Program SPP 1362 “Porous Metal–Organic Frameworks”, organized by S. Kaskel, and part of the EU 7th Framework project M_4CO_2, organized by F. Kapteijn and J. Gascon. Profs. Krishna (Amsterdam) and Feldhoff (Hannover) are thanked for stimulating discussions. We are especially thankful to Christian Ostertag-Henning and Jürgen Poggendorf from BGR Hannover for the mass spectrometric analysis. Additionally we thank TU Delft for manufacturing the permeation cells for our measurements.

References

[1] S. Kaufmann, W.F. Libby, Phys. Rev. 93 (1953) 1337–1344.
[2] H.K. Rae, Am. Chem. Soc. 68 (1978) 1–26.
[3] T.X. Nguyen, H. Jobic, S.K. Bhatia, Phys. Rev. Lett. 105 (2010), 085901-1.
[4] J.J.M. Beenakker, V.D. Borman, S.Y. Krylov, Chem. Phys. Lett. 232 (1995) 379–382.
[5] H. Oh, I. Savchenko, A. Mavrandonakis, T. Heine, M. Hirscher, ACSNano 8 (2014) 761–770.
[6] I. Krkljus, T. Steriotis, G. Charalambopoulou, A. Gotzias, M. Hirscher, Carbon 57 (2013) 239–247.
[7] R. Krishna, J. Phys. Chem. C 113 (2009) 19756–19781.
[8] R. Krishna, J.M. van Baten, J. Phys. Chem. C 116 (2012) 23556–23568.
[9] R. Banerjee, H. Furukawa, D. Britt, C. Knobler, M. O'Keeffe, O.M. Yaghi, J. Am. Chem. Soc. 131 (2009) 3875–3877.
[10] A. Torrisi, R.G. Bell, C. Mellot-Draznieks, Cryst. Growth Des. 10 (2010) 2839–2841.
[11] J.-R. Li, R.J. Kuppler, H.-C. Zhou, Chem. Soc. Rev. 38 (2009) 1477–1504.
[12] S. Ma, H.-C. Zhou, Chem. Commun. 46 (2010) 44–53.
[13] J. Teufel, H. Oh, M. Hirscher, M. Wahiduzzaman, L. Zhechkov, A. Kuc, et al., Adv. Mater. 25 (2013) 635–639.
[14] Y. Jiao, A. Du, M. Hankel, S.C. Smith, Phys. Chem. Chem. Phys. 15 (2013) 4832–4843.
[15] D. Zhang, L. Zhou, W. Su, Y. Sun, Chinese J. Chem. Eng. 14 (2006) 526–531.
[16] A. Schulz, F. Steinbach, J. Caro, J. Membr. Sci. 469 (2014) 284–291.
[17] K. Malek, M.O. Coppens, J. Chem. Phys. 119 (2003) 2800–2811.
[18] S.T. Oyama, D. Lee, P. Hacarlioglu, R.F. Saraf, J. Membr. Sci. 244 (2004) 45–53.
[19] A. Huang, W. Dou, J. Caro, J. Am. Chem. Soc. 132 (2010) 15562.
[20] H. Bux, F. Liang, Y. Li, J. Cravillon, M. Wiebcke, J. Caro, J. Am. Chem. Soc. 131 (2009) 16000.
[21] Y. Liu, N. Wang, Z. Cao, J. Caro, J. Mater. Chem. A 2 (2014) 1235–1238.
[22] Y. Liu, N. Wang, J. Caro, J. Mater. Chem. A 2 (2014) 5716–5723.
[23] A. Huang, F. Liang, F. Steinbach, J. Caro, J. Membr. Sci. 350 (2010) 5–9.
[24] S. Khajavi, F. Kapteijn, J.C. Jansen, J. Membr. Sci. 299 (2007) 63–72.
[25] A. Huang, N. Wang, J. Caro, Micropor. Mesopor. Mater. 164 (2012) 294–301.
[26] J.L.C. Rowsell, O.M. Yaghi, J. Am. Chem. Soc. 128 (2006) 1304–1315.
[27] P. Mercea, S. Cuna, St. Kreibik, Isotopenpraxis 26 (1990) 18–22.
[28] P. Agrinier, D. Roizard, M.F. Ruiz-Iopez, E. Favre, J. Membr. Sci. 318 (2008) 373–378.
[29] S. Tanaka, R. Kiyose, J. Nucl. Sci. Technol. 16 (1979) 923–925.
[30] M. Glugla, I.R. Cristescu, I. Cristescu, D. Demange, J. Nucl. Mat. 355 (2006) 47–53.
[31] K. Aoki, S. Yokoyama, K. Kusakabe, S. Morooka, Korean J. Chem. E 13 (1996) 530–537.
[32] A.F.P. Ferreira, M.C. Mittelmeijer-Hazeleger, A. Bliek, Adsorption 13 (2007) 105–114.
[33] M. Fernandez, J. Kärger, F. Freude, A. Pampel, J.M. van Baten, R. Krishna, Micropor. Mesopor. Mater. 105 (2007) 124–131.
[34] R. Krishna, J.M. van Baten, Chem. Eng. J. 140 (2008) 614–620.
[35] R. Krishna, Micropor. Mesopor. Mater. 185 (2014) 30–50.
[36] R. Krishna, J.M. van Baten, J. Membr. Sci. 430 (2013) 113–128.
[37] R. Krishna, Chem. Soc. Rev. 41 (2012) 3099–3118.
[38] A.V.A. Kumar, H. Jobic, S.K. Bhatia, Adsorption 13 (2007) 501–507.
[39] J. Hedlund, J. Sterte, M. Anthonis, A.-J. Bons, B. Carstensen, N. Corcoran, D. Cox, H. Deckman, W. de Gijnst, P.-P. de Moor, F. lai, J. McHenry, W. Mortier, J. Reinoso, J. Peters, Micropor. Mesopor. Mater. 52 (2002) 179–189.
[40] H. Voß, A. Diefenbacher, G. Schuch, H. Richter, I. Voigt, M. Noack, J. Caro, J. Membr. Sci. 329 (2009) 11–17.